Appl Phys A (2010) 99: 465–469
DOI 10.1007/s00339-010-5547-x

Applied Physics A
Materials Science & Processing

Low thermal expansion behavior and transport properties of Ni and Ge co-doped manganese nitride materials at cryogenic temperatures

Rongjin Huang · Xinxin Chu · Zhixiong Wu · Laifeng Li · Xiangdong Xu

Received: 29 June 2009 / Accepted: 6 January 2010 / Published online: 29 January 2010

Abstract A series of Ni and Ge co-doped manganese nitride materials were fabricated by mechanical ball milling followed by solid-state sintering. Their thermal expansion properties and electrical and thermal conductivities were investigated in the temperature range of 77–300 K. The results show that Ni and Ge co-doped manganese nitride materials have negative thermal expansion (NTE), and the operation-temperature window of NTE shifts toward the lower temperature region and the variation of linear thermal expansion ($\Delta L/L_{(300\mathrm{K})}$) in the operation-temperature window of NTE decreases with increasing Ni content. The combination of these two factors results in a low coefficient of thermal expansion (CTE) at cryogenic temperatures. The average CTE of $Mn_3(Cu_{0.2}Ni_{0.4}Ge_{0.4})N$ drops to 'zero' in the temperature range of 190–77 K. The values of electrical and thermal conductivities of the Ni and Ge co-doped manganese nitride materials are in the ranges of 2–3 $\times$ 10^3 $(\mathrm{ohm\,cm})^{-1}$ and 1.6–3.4 $\mathrm{W\,(m\,K)^{-1}}$, respectively.

1 Introduction

In cryogenic engineering, structural systems undergo thermal shock when the temperature varies between room temperature and cryogenic temperature. A low-temperature structure consisting of materials with different thermal expansions will have a residual stress distribution and deformation after it is cooled and warmed. The performance of a high-precision device has been limited by the problems induced by the thermal expansion between different materials. For example, the refrigeration efficiency of a piston refrigerator will be decreased when the piston to cylinder wall clearance changes, caused by the different coefficients of thermal expansion (CTE) of piston and cylinder. Microelectronics and micro-electro-mechanical systems in space may be limited by thermal stress problems induced by thermal expansion. To avoid these problems, one of the possible methods is the development of very low thermal expansion material.

Very low thermal expansion has been reported for some alkali–zirconium phosphates [1], such as $PbM_{1/3}Nb_{2/3}O_3$ [2], $MTi_2(PO_4)_3$ (M = Li, Na, K) [3, 4], $MZr_4P_6O_{24}$ (M = Mg, Ca, Sr, Ba) [5, 6], amorphous SiO_2 and a few Invar alloys [7–9]. However, except for the Invar alloys, most of the low thermal expansion materials are insulators, which are of limited use in some electrical devices. Thus, there is a need for new materials with very low thermal expansion but that are capable of conducting electric current [10]. The recent development of giant negative thermal expansion in Ge- or Sn-doped materials, $Mn_3(Cu_{1-x}Ge_x)N$ and $Mn_3(Cu_{1-x}Sn_x)N$, has rekindled interest in studying the thermal expansion properties of anti-perovskite manganese nitrides [11–14]. Mn_3AN is an interstitial compound and has a cubic crystal structure with space group $Pm3m$. The Mn and N atoms are located at the face centered and body centered positions, respectively. The A ion sits on a cubic lattice and is less bound to N [15], which allows the introduction of various metals on the site of A [16]. It was reported that a small substitution on A can affect the thermal expansion property of Mn_3AN [17]. It is suggested that low CTE may

R. Huang · X. Chu · Z. Wu · L. Li (✉) · X. Xu
Key Laboratory of Cryogenics, Technical Institute of Physics and Chemistry, Chinese Academy of Sciences, Beijing, P.R. China
e-mail: lfli@mail.ipc.ac.cn

X. Chu · Z. Wu
Graduate University of the Chinese Academy of Sciences, Beijing, P.R. China

be obtained by a substitution on A. We note that the element Ni is located at the left of Cu in the periodic table of the elements; Ni is assumed to have similar chemical properties to Cu. This prompts us to investigate manganese nitride material with partial substitution of Ni and Ge for Cu.

In the present study, bulk materials with the general formula $Mn_3(Cu_{0.6-x}Ni_xGe_{0.4})N$ ($x = 0$, 0.1, 0.15, 0.2, 0.25, 0.3, 0.35, 0.4) were fabricated by mechanical ball milling followed by solid-state sintering. A structural study was performed using X-ray diffraction. Their thermal expansion properties and electrical and thermal conductivities were investigated in the temperature range of 77–300 K.

2 Experimental

The studied polycrystalline samples with the general formula $Mn_3(Cu_{0.6-x}Ni_xGe_{0.4})N$ ($x = 0$, 0.1, 0.15, 0.2, 0.25, 0.3, 0.35, 0.4) were prepared by a solid state reaction method. The powders of Cu (99.99 at.% pure), Ni (99.99 at.% pure), Ge (99.999 at.% pure) and Mn (99.99 at.% pure) with initial particle size of about ~0.01 mm were used as the starting materials. Firstly, Mn_2N powders were synthesized by flowing purified nitrogen gas into pure Mn powders at 750°C for 60 h. Then, the powders of Cu, Ni, Ge and Mn_2N are charged into agate jars with agate balls under a purified argon atmosphere. Mechanical ball milling was conducted in a planetary ball mill at the rotating speed of 350 rpm for 24 h. The as-milled powders were preformed under a pressure of 500 MPa at room temperature. The preformed samples were wrapped with tantalum foil and sintered at 850°C under a purified argon atmosphere for 48 h.

The crystal structures and phase constitutions of the samples were characterized at room temperature by X-ray diffraction (XRD) analysis using a Rigaku D/max-RB diffractometer with Cu K_α radiation ($\lambda = 0.154056$ nm). Morphological characterization was performed by scanning electron microscopy (SEM). The linear thermal expansion data ($\Delta L/L_{(300K)}$) was measured using strain gauges over the temperature range of 77–300 K. (Note that, for sintered polycrystalline samples, $\Delta L/L$ is related directly to the volume expansion in a manner $\Delta L/L = \Delta V/3V$.) As mentioned in [11], the measurement of the linear thermal expansion in this way requires a reference material with known thermal expansion. We used fused silica and the corresponding thermal expansion data [18]. The electrical conductivity was measured using a standard four-probe method in the temperature range of 77–300 K. The thermal conductivity was measured by means of a heat and sink steady state method by establishing a stationary temperature gradient, and supplying heat at one end of the sample while the other end is maintained at a constant temperature. By measuring the temperature difference between given distances, the temperature difference of the two ends of the sample was stabilized with an accuracy of better than 1×10^{-2} K. The thermal conductivity could be calculated by means of

$$K = \dot{Q}\frac{L}{S\Delta T}, \tag{1}$$

where $\dot{Q}$ is the power supplied, L the distance of the sample, S the section of the sample, ΔT the measured temperature difference and K the thermal conductivity.

3 Results and discussion

3.1 Structures

The indexed XRD patterns for $Mn_3(Cu_{0.6-x}Ni_xGe_{0.4})N$ ($x = 0$, 0.1, 0.2, 0.3, 0.4) samples at room temperature are given in Fig. 1. The XRD patterns show that these samples have a dominating phase with the Mn_3CuN-type structure (space group, $Pm3m$) (JCPDS card, PDF#23-0220). However, other diffraction peaks were found in the samples doped with Ni and Ge. The relative intensities of diffraction peaks, corresponding to a 2θ angle of about 44.5°, increase with the increase of Ni content. These diffraction peaks derived from the manganese–nickel alloy (JCPDS card, PDF#54-0553). It can therefore be estimated that much more existence of manganese–nickel might have an influence on the thermal expansion property and other physical properties. Figure 2 shows a SEM image of $Mn_3(Cu_{0.2}Ni_{0.4}Ge_{0.4})N$. It is clear that some small pores remain inside the sample. These pores may result from the release of excessive nitrogen in the stage of sintering.

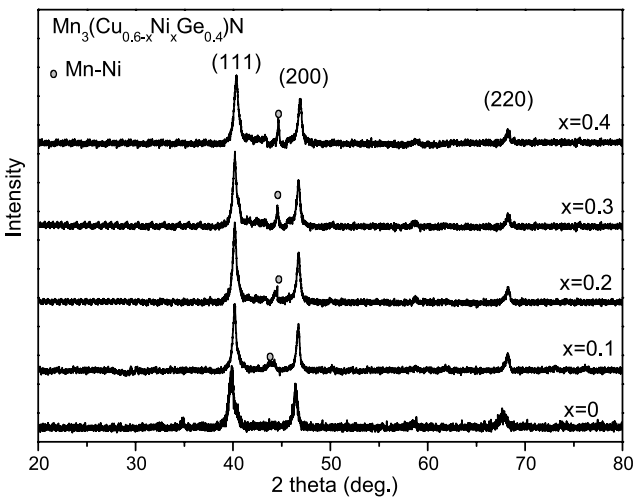

Fig. 1 X-ray diffraction patterns of $Mn_3(Cu_{0.6-x}Ni_xGe_{0.4})N$ ($x = 0$, 0.1, 0.2, 0.3, 0.4) at room temperature

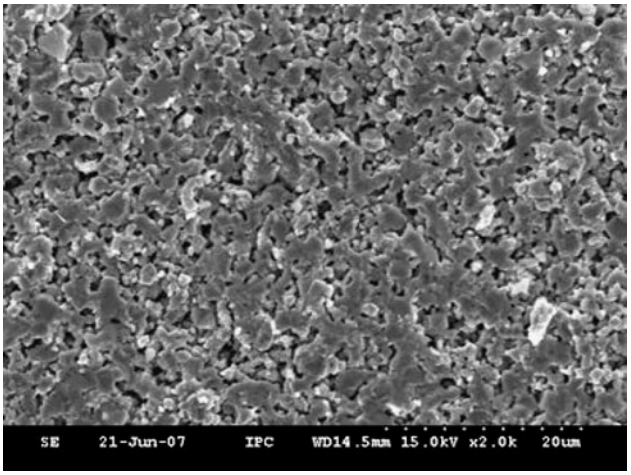

Fig. 2 SEM image of $Mn_3(Cu_{0.2}Ni_{0.4}Ge_{0.4})N$

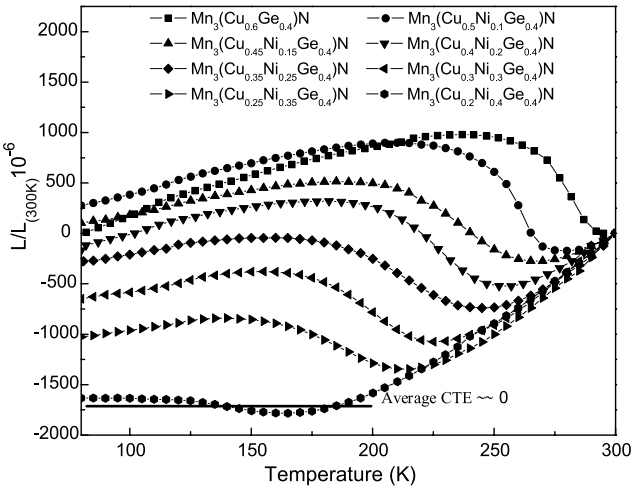

Fig. 3 Linear thermal expansion coefficients of $Mn_3(Cu_{0.6-x}Ni_x Ge_{0.4})N$ ($x = 0$, 0.1, 0.15, 0.2, 0.25, 0.3, 0.35, 0.4) in the temperature range of 77–300 K

3.2 Thermal expansion properties

The linear thermal expansion data ($\Delta L/L_{(300K)}$) obtained for samples $Mn_3(Cu_{0.6-x}Ni_xGe_{0.4})N$ ($x = 0$, 0.1, 0.15, 0.2, 0.25, 0.3, 0.35, 0.4) are shown in Fig. 3. It can be seen that for each sample there exists a temperature region in which the linear thermal expansion increases with decreasing temperature, i.e. negative thermal expansion (NTE) occurs. However, the operation-temperature window of NTE changes with varying Ni and Ge contents. The sample $Mn_3(Cu_{0.6}Ge_{0.4})N$ without Ni doping displays NTE behavior around room temperature (295–245 K). On increasing the amount of Ni from 0.1 to 0.4, the operation-temperature window of NTE moves constantly toward the lower temperature region. It suggests that the operation-temperature window of NTE is affected by the partial substitution of Ni and Ge for Cu. It was reported that the magnetovolume effect is responsible for the negative thermal expansion in Mn_3AN. The magnetic transition temperature of Mn_3AN is affected by the 'electron concentration' around element A [17]. We notice that the electronic shell of Ni is [Ar] $3d^84s^2$, while for Cu the electronic shell is [Ar] $3d^{10}4s^1$. It means that Ni will have fewer free electrons than Cu in Mn_3AN at a given temperature. So, the 'electron concentration' will decrease when we partially substitute Ni and Ge for Cu. As a result, with increasing Ni content, the operation-temperature window of NTE shifts toward the lower temperature region.

Furthermore, another important feature to be stressed is that the magnitude of the negative thermal expansion is affected by the Ni content. The variation of $\Delta L/L_{(300K)}$ in the temperature region of NTE decreases with the increase of Ni content. For example, the variation of $\Delta L/L_{(300K)}$ of $Mn_3(Cu_{0.6}Ge_{0.4})N$ is about 1032×10^{-6}, while for the samples $Mn_3(Cu_{0.4}Ni_{0.2}Ge_{0.4})N$ and $Mn_3(Cu_{0.3}Ni_{0.3}Ge_{0.4})N$ it is 841×10^{-6} and 704×10^{-6}, respectively. Especially for $Mn_3(Cu_{0.2}Ni_{0.4}Ge_{0.4})N$, at temperature $T > 165$ K, the linear thermal expansion is linear in T and the slope decreases gradually with decreasing temperature, which is nearly consistent with the Grüneisen formula. Within the temperature range of 125–165 K, the linear thermal expansion $\Delta L/L_{(300K)}$ data increase with decreasing temperature, indicating that NTE behavior occurs, but the variation of $\Delta L/L_{(300K)}$ is only 100×10^{-6}. When the temperature $T < 125$ K, $Mn_3(Cu_{0.2}Ni_{0.4}Ge_{0.4})N$ keeps the value of $\Delta L/L_{(300K)}$ nearly constant. If the variation of $\Delta L/L_{(300K)}$ is considered from 190 to 77 K, we will have the average CTE $\bar{\alpha} = 3.4 \times 10^{-6}$ K^{-1} in the temperature range of 190–165 K, -3.2×10^{-6} K^{-1} in 165–125 K, 0.6×10^{-6} K^{-1} in 125–77 K and 'zero' in the temperature of 190–77 K; see the level line in Fig. 3. These data indicate that $Mn_3(Cu_{0.2}Ni_{0.4}Ge_{0.4})N$ material has excellent volume stability in the temperature range of 190–77 K ($\Delta = 113$ K).

A very recent paper [19] on doped manganese nitride material has found zero thermal expansion materials, which consist of a pure-form anti-perovskite manganese nitride obtained by optimizing the nitrogen content, such as $Mn_3(Cu_{0.5}Sn_{0.5})N_{1-\delta}$. It is suggested that the nitrogen deficiency is one of origins of the decrease in the negative slope of $\Delta L/L$. However, this seems unlikely to be the case for our samples, $Mn_3(Cu_{0.6-x}Ni_xGe_{0.4})N$. We found manganese–nickel alloy distributed in the Ni and Ge co-doped manganese nitride material. Furthermore, it is clearly seen from Fig. 1 that the relative intensities of diffraction peaks derived from the manganese–nickel alloy increase with increasing Ni, indicating that the content of manganese–nickel alloy increases with molar fraction x. Manganese nitride material shows negative thermal expansion in the operation-temperature window of NTE, while the manganese–nickel may show normal positive thermal expansion. The thermal expansion properties of the Ni and

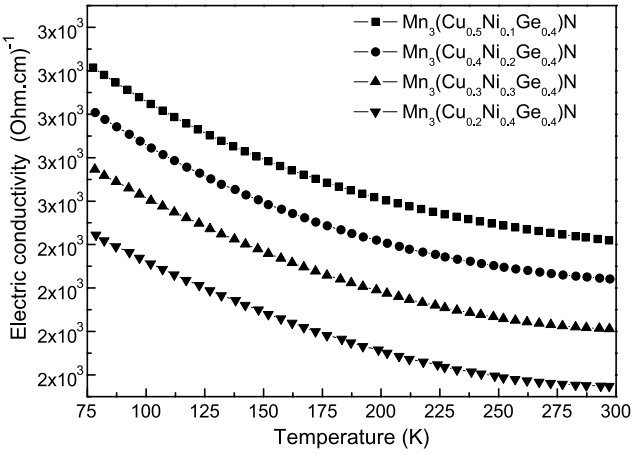

Fig. 4 The electrical conductivities of $Mn_3(Cu_{0.6-x}Ni_xGe_{0.4})N$ ($x = 0.1, 0.2, 0.3, 0.4$) in the temperature range of 77–300 K

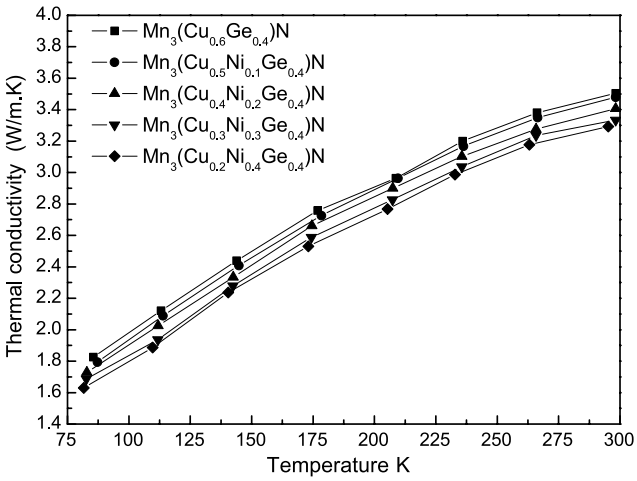

Fig. 5 The thermal conductivities of $Mn_3(Cu_{0.6-x}Ni_xGe_{0.4})N$ ($x = 0, 0.1, 0.2, 0.3, 0.4$) in the temperature range of 77–300 K

Ge co-doped manganese nitride materials with distribution of manganese–nickel alloy may originate from a combination of negative expansion in the manganese nitride and positive expansion in the impurities. As the manganese–nickel alloy content increases, the CTE of the composite decreases. When $x = 0.4$, $Mn_3(Cu_{0.2}Ni_{0.4}Ge_{0.4})N$ shows very low CTE. To obtain further insight into the mechanism of low thermal expansion in Ni and Ge co-doped manganese nitride material, a much more detailed quantitative investigation of the amounts of various crystal phases and their thermal expansions will be carried out.

3.3 Electrical and thermal conductivities

The materials that exhibit low thermal expansion are almost all insulators. However, for many applications, the capability of conducting electric current by materials with very low thermal expansion behavior must be considered [11]. Figure 4 shows the temperature dependence of electrical conductivities for $Mn_3(Cu_{0.6-x}Ni_xGe_{0.4})N$ ($x = 0.1$, 0.2, 0.3, 0.4). It is clear that the electrical conductivities decrease monotonically with increasing temperature in the whole measuring temperature range, being characteristic of a metal. Furthermore, it is obvious that the electrical conductivities decrease with the increase of Ni content, but are independent of NTE behaviors. The values of the electrical conductivities are in the range of 2–3 $\times 10^3$ $(\text{ohm cm})^{-1}$. Thermal conductivity is also one of the important physical parameters for applications. High thermal conductivity is desirable for some cryogenic applications in order to keep a homogeneous temperature to avoid stresses. In this study, we investigated the thermal conductivities of $Mn_3(Cu_{0.6-x}Ni_xGe_{0.4})N$ ($x = 0$, 0.1, 0.2, 0.3, 0.4) in the temperature range of 77–300 K. Figure 5 shows the thermal conductivities as a function of temperature for samples $Mn_3(Cu_{0.6-x}Ni_xGe_{0.4})N$ ($x = 0$, 0.1, 0.2, 0.3, 0.4). It is clear that the thermal conductivities increase monotonically with increasing temperature in the whole measurement temperature range. Furthermore, it is obvious that the thermal conductivity decreases with the increase of Ni content. It can be attributed to the fact that the thermal conductivity of Ni is lower than that of Cu. The thermal conductivities of all samples are also independent of NTE behaviors. The values of the thermal conductivities are in the range of 1.6–3.4 W (m K)^{-1}. The transport properties of the samples highly depend on sintering conditions of the samples. The electrical and thermal conductivities are relatively low due the pores remaining inside the samples (Fig. 2). If the samples are synthesized by hot-press sintering, the electrical and thermal conductivities should be improved. On the other hand, microcracks may be generated in the samples at every thermal cycle, which affect the transport properties [20]. The stability of the conductivity will be further investigated.

4 Conclusion

In this study, Ni and Ge co-doped manganese nitride materials were synthesized by mechanical alloying followed by solid-state sintering. Their crystal structures, thermal expansion properties and electrical and thermal conductivities were investigated. X-ray diffraction analyses confirmed that all samples have a dominating phase with the Mn_3CuN-type structure, but a second phase of manganese–nickel alloy was found. The operation-temperature window of NTE shifts toward lower temperatures and the variation of $\Delta L/L_{(300\text{K})}$ in the temperature region of NTE decreases with the decrease of Ni content. The combination of these two factors resulted in low CTE at cryogenic temperatures. $Mn_3(Cu_{0.2}Ni_{0.4}Ge_{0.4})N$ shows 'zero' average CTE in the temperature range of 190–77 K. The values of electrical

conductivities and thermal conductivities are in the ranges of 2–3 $\times$ 10^3 $(\mathrm{ohm\,cm})^{-1}$ and 1.6–3.4 $\mathrm{W\,(m\,K)^{-1}}$, respectively, and independent of NTE behaviors. This Ni and Ge co-doped manganese nitride material may possibly be exploited to design critical components in cryogenic engineering and aerospace areas.

Acknowledgements This project is supported by the National Natural Science Foundation of China (Nos. 10904153 and 50676101) and the CAS Chinese Overseas Outstanding Scholar Foundation (2006-1-17).

References

1. G.E. Lenain, S.Y. Limaye, H.A. McKinstry, A. Woodward, Mater. Res. Bull. **19**, 1451–1456 (1984)
2. D.K. Agrawal, R. Roy, H.A. McKinstry, Mater. Res. Bull. **22**, 83–88 (1987)
3. D.A. Woodcock, P. Lightfoot, J. Mater. Chem. **9**, 2907–2911 (1999)
4. D.A. Woodcock, P. Lightfoot, C. Ritter, Chem. Commun. **1**, 107–108 (1998)
5. S.Y. Limaye, D.K. Agrawal, H.A. McKinstry, J. Am. Ceram. Soc. **70**, 232–236 (1987)
6. T. Ota, P. Jin, I. Yamai, J. Mater. Sci. **24**, 4239–4245 (1989)
7. W.D. Kingery, H.K. Bowen, D.R. Uhlmann, *Introduction to Ceramics* (Wiley, New York, 1976)
8. K. Lagarec, D.G. Rancourt, Phys. Rev. B **62**, 978–985 (2000)
9. G. Hausch, R. Bächer, J. Hartmann, Physica B **161**, 22–24 (1989)
10. J.R. Salvador, F. Guo, T. Hogan, M.G. Kanatzidis, Nature **425**, 702–705 (2003)
11. K. Takenaka, H. Takagi, Appl. Phys. Lett. **87**, 261902 (2005)
12. K. Takenaka, K. Asano, M. Misawa, H. Takagi, Appl. Phys. Lett. **92**, 011927 (2008)
13. K. Takenaka, H. Takagi, Mater. Trans. **47**, 471–474 (2006)
14. S. Iikubo, K. Kodama, K. Takenaka, H. Takagi, S. Shamoto, Phys. Rev. B **77**, 020409 (2008)
15. J. Garcíaa, J. Bartoloméa, D. González, R. Navarrob, D. Fruchart, J. Chem. Thermodyn. **15**, 465–473 (1983)
16. Y. Sun, C. Wang, Y. Wen, K. Zhu, J. Zhao, Appl. Phys. Lett. **91**, 231913 (2007)
17. D. Fruchart, E. Bertaut, J. Phys. Soc. Jpn. **44**, 781–791 (1978)
18. R.K. Kirby, T.A. Hahn, *NIST Standard Reference Material 739, Fused-silica Thermal Expansion. Certificate of Analysis* (National Institute of Standards and Technology, Washington, 1971)
19. K. Takenaka, H. Takagi, Appl. Phys. Lett. **94**, 131904 (2009)
20. W.S. Kim, E.O. Chi, J.C. Kim, N.H. Hur, K.W. Lee, Y.N. Choi, Phys. Rev. B **68**, 172402 (2003)